*

Enhancing the efficiency of solar pond heat extraction by using both lateral and bottom heat exchangers

A. Alcaraz[1], C. Valderrama[1], J. L. Cortina[1], A. Akbarzadeh[2], A. Farran[1]

[1]Departament d'Enginyeria Química, Universitat Politècnica de Catalunya-Barcelona TECH

[2]Energy Conservation and Renewable Energy Group, School of Engineering, RMIT University

*Correspondence should be addressed to: César Valderrama

Departament d'Enginyeria Química, Universitat Politècnica de Catalunya-Barcelona TECH

Av. Diagonal 647, 08028, Barcelona Spain

Tel.: 93 4011818, Fax.: 93 401 58 14

Email: cesar.alberto.valderrama@upc.edu

Abstract

In this study, heat extraction from both the gradient and heat storage zones of a salinity-gradient solar pond (SGSP) has been evaluated. For this purpose, an experimental solar pond pilot plant was constructed in 2009 in Barcelona (Spain). The structure of the pond is a cylindrical tank of 3-m height and 8 m diameter with a total area of 50 m^2. The main objective was to evaluate a heat-extraction system from the SGSP designed to enhance the system efficiency under different conditions. Thus, an in-pond heat exchanger covering all of the lateral wall area of the pond was installed, and its performance was compared with the traditional in-pond heat exchanger situated on the bottom of the pond. Heat extraction experiments were performed using both heat exchangers individually or both at the same time. The study covers the experiments performed at three different seasonal temperature conditions: winter (December), summer (July) and autumn (October and November). The variations of the temperature inside the pond during the heat extraction were measured and analyzed. The results demonstrated that the efficiency of the pond

increases when the heat is removed from the lateral heat exchanger alone compared to either using the bottom heat exchanger or using both heat exchangers simultaneously.

Keywords: energy storage; solar radiation; solar pond; heat extraction; efficiency

1. Introduction

Renewable energy resources and technologies have a key role to play in meeting current and future energy needs, as well as in minimizing the depletion of non-renewable fuels and the environmental consequences of climate change. During the past decades, solar energy sources have gained greater importance in meeting the energy demands for various sectors. Among the different options, the solar pond is one alternative as a thermal energy storage systems. A solar pond was discovered as a natural phenomenon during the last century in Medve Lake in the Transylvania region in Romania. In this lake, temperatures up to 70°C were recorded at a depth of 1.32 m at the end of the summer season (El-Sebaii et al., 2011; Bozkurt and Karakilcik, 2015). In practice, any pond with a black bottom is capable of collecting solar energy, but the collection efficiency is poor because heated water at the bottom rises by convection to the top, where the heat is rapidly dissipated to the environment. The convection currents can be minimized by the presence of a strong density gradient from bottom to top (Weinberger, 1964; Bansal and Kaushik, 1981). This density gradient can be generated by using a high concentration of a salt such as NaCl at the bottom of the pond and low-salinity water at the top resulting in a configuration called a salinity-gradient solar pond (SGSP). A typical SGSP consists of three distinct zones (Zangrando, 1980; Tabor and Weinberger, 1981). The surface area formed by fresh water or low salinity water is called the upper convective zone (UCZ) and it is a zone of constant temperature close to the ambient air temperature and constant salinity between 2 and 3%. Below this UCZ, there is an intermediate zone consisting of several layers with different densities. The brine density gradually increases towards the bottom of the pond causing a concentration gradient. This gradient prevents the occurrence of convection currents and, as a result of solar energy absorption, a gradient of temperature is also established. The gradient zone is known as the non-convective zone (NCZ) and it is the key to this technology. The lower zone has the highest density (near saturation) and is known as the low convective zone (LCZ). This zone acts as a thermal storage with temperature ranging between 50 and 90°C, depending on both the size of the pond and the weather parameters.

The heat accumulated in the SGSP has been conventionally extracted from the LCZ using two methods. The first method is by withdrawing the hot brine from the upper region of LCZ by means of a diffuser to prevent excessive velocities of motion within the pond and thereby minimizing the erosion of the gradient zone. The heat of the brine is removed by an external heat exchanger, and the cooled brine is returned to the pond on the other end (Leblanc et al., 2011). This method has been used in several solar ponds worldwide as in El Paso (Texas, USA) (Xu et al., 1993), Kutch (India) (Kumar and Kishore, 1999), Beith Ha'rava (Israel) (Tabor and Doron, 1990) and Singapore (Kho et al., 1991). In the second method, an in-pond heat exchanger placed in the LCZ is used to remove the heat from this storage zone and to transfer its thermal energy for use in heating buildings, power production and industrial processing (Akbarzadeh et al., 2005). This method has been proven by several solar pond studies such as in Pyramid Hill (Victoria, Australia) (Leblanc et al., 2010), Marshad (Iran) (Jaefarzadeh, 2006) and at The Ohio State University (USA) (Nielsen, 1980). This method of heat extraction has several disadvantages, such as the large number of tubes required, the difficulty of repairing them and corrosion problems (El-Sebaii et al., 2011).

The possibility of an alternative method of heat extraction from the NCZ, i.e., the gradient layer of a solar pond as well as or instead of the conventional extraction from LCZ, was explored in a theoretical study by Andrews and Akbarzadeh (2005). An experimental study of this novel heat-extraction method was performed over a period of two months and was compared with theoretical analysis (Leblanc et al., 2011). The results indicated that heat extraction from the gradient layer increases the overall energy efficiency of the solar pond by up to 55%, compared with heat extraction from the LCZ (Ranjan and Kaushik, 2014).

Other studies reported a steady-state and transient theoretical model based on removing the heat stored in the NCZ to improve the thermal efficiency of the pond (Andrews and Akbarzadeh, 2005; Leblanc et al., 2011; Date et al., 2013; Dehghan et al., 2013) or withdrawing hot brine from the different layers of the gradient zone (Yaakob et al., 2011). However, few data about experimental heat extraction through the NCZ or focussing on the simultaneous heat extraction using both heat exchange methods have been reported. In view of this, the aim of this study is to evaluate an alternative system of heat extraction from a salinity-gradient solar pond to enhance the thermal efficiency of the system. Thus, an in-pond heat exchanger covering the pond wall (NCZ and LCZ) was used and compared with the traditional heat-extraction method using an in-pond heat exchanger placed at the bottom of the pond. Experiments were performed during three different seasons of the year covering an ambient temperature range from 10 to 30°C. Moreover, to explore the potential to enhance the overall efficiency of the solar pond, experiments using both heat exchangers were also performed.

2. Materials and methods

2.1 Solar pond description

The solar pond pilot plant located in Martorell (Barcelona, Spain) has a surface area of 50 m^2 and a depth of 3 m. The level of the water in the pond was fixed at 2.6 m by using an overflow system. The thicknesses of the LCZ, NCZ and UCZ were approximately 0.55, 1.35 and 0.7 m, respectively. The walls and bottom of the pond were insulated to prevent heat losses. The lateral pond wall was insulated with 60 mm of rock wool and then covered with 0.8 mm of smooth aluminium plates. The bottom area was insulated with 40 mm of polystyrene and then covered with a concrete slab with a thickness of 150 mm. The inner surface of the concrete was coated with Remmers Aida® Kiesol to waterproof and protect the concrete against corrosion. The pond was above the ground; thus, it was necessary to build a stairway to gain access to the sampling system, salt charger and overflow system. A mobile sampling mechanism was implemented to measure density, pH and turbidity at different heights (every 10 cm of height) (Jaefarzadeh and Akbarzadeh, 2003; Valderrama et al., 2011). A portable density meter DMA 35 (Anton Paar, accuracy: ± 0.001 g/cm^3) was used for measurement of density. The storage zone contains saturated brine of approximately 25% NaCl by weight. The UCZ concentration is 1 to 3 (% wt.) salt. A typical density profile of the Martorell solar pond during a 12-month period is shown in Figure 1. The pH and turbidity were measured by a portable pH meter (Crison pH25, accuracy: ± 0.01 pH) and portable turbidity meter (Hanna HI93703C, accuracy: ± 0.5 NTU).

Figure 1.

The temperature measurements at different solar pond heights were performed by means of 21 sensors (PT-100 K-type thermoresistances, Abco, Spain) distributed at a spacing of every 14 cm (starting at 0.5 cm from the bottom) and installed in a plastic support fixed to the pond wall.

The solar radiation (W/m^2) was measured at time intervals of 10 s (CS300, Apogee SP-110 silicon photocell pyranometer with an uncertainty of ± 5%) and was recorded using an automatic measurement and control system (Campbell Scientific, Barcelona, Spain) which was programmed to measure and store data (Datalogger CR1000). Details of the solar pond construction, monitoring and gradient settling can be found elsewhere (Valderrama et al., 2011). A view of the experimental Martorell solar pond is shown in Figure 2.

Figure 2.

2.2 Heat-extraction system

The heat-extraction system is composed of a cooler system (HRS024-AF-20 2.1kW SMC) and two heat exchangers. The first one is located in the LCZ, and the second heat exchanger covers the pond wall from 0.10 m to 2.70 m above the bottom (Figure 3). Both in-pond heat exchangers are made of polybutylene pipe with an internal diameter of 26 mm, an external diameter of 30 mm and a thermal conductivity of approximately 0.22 W/(m·K). The bottom and lateral heat exchangers are 250 m and 730 m in length, respectively (Figure 3a). A heat-transfer fluid circulates in a closed loop through the internal heat exchangers. Depending on the heat exchanger used, the heat will be extracted from a specific zone of the pond, that is, the bottom, lateral or both bottom and lateral zones. The temperature of the fluid in the inlet and outlet pipes of each heat exchanger was measured by thermal sensors (PT100) and the flow rate was controlled by a flow meter (SMC) located in the inlet and the outlet pipes of both the heat exchangers. A schematic diagram of the heat-extraction system is shown in Figure 3b.

Figure 3.

The cooler is an air-cooled system formed by two circuits, the working fluid circuit and the refrigerant circuit. The working fluid, water in this case, runs through the circuit removing the heat from the solar pond. The refrigerant is a high-temperature and high-pressure gas that flows through the closed refrigerant circuit and cools the working fluid.

When the heat is extracted by the heat exchanger in the LCZ, the water flows through the pipe at the bottom of the pond removing heat from the LCZ (Figure 3b). The fluid then exits the pond at a temperature near the temperature of the storage zone of the pond, to be cooled by the cooler system. The water, after being cooled, is then pumped back to the pond to start a new cycle. In the case of the lateral heat exchanger (Figure 3c), the fluid flows through the pipe from the top (at the boundary between the UCZ and the NCZ) to the bottom of the pond along the lateral heat exchanger, extracting heat through the NCZ and the LCZ, then exiting the pond at a temperature near the temperature of the storage zone, then to be cooled by the cooler system. In both heat extraction methods, the working fluid passes slowly through the cooler layers of the NCZ and the UCZ causing a decrease of the temperature due to the temperature difference between the LCZ and the upper regions of the NCZ and the UCZ.

3. Efficiency and effectiveness of a solar pond

Many authors have defined the efficiency of the solar pond from the point of view of thermal energy stored in the system relative to the incident radiation on the pond (Bozkurt and Karakilcik, 2015; Karakilcik et al., 2006; Dehghan et al., 2013). Nevertheless, a solar pond would make sense only when the heat extraction process is performed because the system is not only capable of storing thermal energy but also of supplying thermal energy to a particular application. Therefore, other studies have focused on defining solar pond efficiency as the ratio of the extracted energy and the incident radiation (Andrews and Akbarzadeh, 2005; Leblanc et al., 2011).

Indeed, using only the heat extraction rate to calculate the efficiency of the system can be misleading. The more common definition of the solar pond is a system which is capable of collecting solar radiation and storing this energy in the form of heat (Tabor and Weinberger, 1981; Hull et al., 1989) to supply this heat at a low temperature to a particular application. Accordingly, the instantaneous efficiency concept introduced by Date et al., 2013 was used in this work. The instantaneous efficiency is defined as the instantaneous change in the energy content of the LCZ divided by the daily average solar radiation that penetrates the top surface of the solar pond during the heat extraction process. The instantaneous energy change can be calculated as the sum of the heat extracted from the solar pond and solar energy absorbed in the LCZ in a time interval (Eq.1).

$$\Delta E_{lcz}^{\tau} = j_{mf}\ C_{p\,f}\left(T_{o\,f}^{\tau} - T_{i\,f}^{\tau}\right)\Delta\tau + X_{lcz}\,A_{sp}\,\rho_{lcz}\,C_{p\,lcz}\left(T_{lcz}^{\tau} - T_{lcz}^{\tau-1}\right) \tag{1}$$

where $j_{m\,f}$ is the mass flux of the heat transfer fluid (kg/(m^2·s)), $C_{p\,f}$ is the specific heat capacity of the heat transfer fluid (J/kg·°C), T_{of}^{τ} and $T_{i\,f}^{\tau}$ are the outlet and inlet temperature of the heat transfer fluid (°C), respectively, $\Delta\tau$ is the time increment of the heat extraction process (s), X_{lcz} is the path length of light in the solar pond to the end of the LCZ (m); and A_{sp} and ρ_{lcz} are the surface area of solar pond (m^2) and the density of the brine in the LCZ (kg/m^3), respectively.

$C_{p\,lcz}$ is the specific heat capacity of the brine solution in the LCZ (J/kg·°C), whereas $T_{lcz}^{\tau-1}$ and T_{lcz}^{τ} are the LCZ temperature at the beginning and the end of the heat extraction process (°C), respectively. Hence, the instantaneous efficiency of the solar pond ($\eta_{inst\ SP}$) can be calculated by using Eq. 2 where $\overline{H}$ is the total energy of the solar radiation incident on the horizontal surface of the pond (MJ/m^2)

$$\eta_{inst\ SP} = \frac{\Delta E_{lcz}^{\tau}}{A_{sp}\ H^{\tau}} \tag{2}$$

The specific heat capacity of the salt solution (kJ/kg·K) is given by Eq. 3 (Wang and Akbarzadeh, 1982) where S is the salt concentration (kg/m^3). The density in the LCZ, ρ_{LCZ}, is the density measured at this height as it was described in section 2.1:

$$C_{p\,lcz} = 4180 + 4.396S + 0.0048S^2 \tag{3}$$

Furthermore, the effectiveness of the heat exchanger can also be determined according to Eq. 4 (Tundee et al., 2010):

$$\varepsilon = \frac{T_{o\,f} - T_{i\,f}}{T_{LCZ} - T_{i\,f}} \tag{4}$$

4. Heat extraction experiments from the solar pond

Three different heat extraction scenarios were experimentally evaluated during three different seasons: heat extraction from i) the lateral heat exchanger (LHE), ii) the bottom heat exchanger (BHE) and iii) simultaneous extraction from the bottom and lateral heat exchangers (BHE + LHE). Each experiment was performed during the daytime over a period of approximately 5 h. The results are reported for each season for the sake of comparison between different scenarios.

4.1 Heat extraction experiments during a cold month (average daily maximum temperature in the range 5 to 10°C)

The heat extraction during the winter was conducted in December 2013. The daily average of the LCZ, the ambient temperature and the average daily solar radiation flux during this month are represented in Figure 4. As can be seen, the maximum daily solar radiation was 5 MJ/m^2, while the average monthly maximum ambient temperature was 7°C. The LCZ temperature decreased during this month from 31.4°C to 24.7°C.

Figure 4.

The experimental conditions of the heat extraction, the effectiveness of each heat exchanger and the instantaneous efficiency of the solar pond are summarized in Table 1. The LCZ temperature during the heat extraction process was approximately 28°C. The mass flow rate in each heat extraction experiment was 0.014 kg/s for both heat exchangers working independently. In the case of simultaneous heat extraction, the total mass flow rate was 0.028 kg/s. The inlet and outlet temperatures of the working fluid were constant with values of approximately 11°C and 23°C, respectively.

The inlet temperature of the working fluid (water) was near the ambient temperature, and the outlet temperature of the working fluid reported similar values independent of the heat-extraction method used. The outlet temperature was 6°C lower than the LCZ temperature in each heat extraction test due to the lower flow rate used. The working fluid passes slowly through the cooler layers of the NCZ and the UCZ causing a decrease in temperature. For this reason, the effectiveness of the three heat extraction methods reported values of 68, 69 and 64%, respectively (Table 1).

Table 1. Experimental conditions, amount of heat extracted, effectiveness and instantaneous efficiency in the heat extraction process during December 2013 (average daily maximum temperature in the range 5 to 10°C).

December 2013		**m (kg/s)**	**T_{in} (°C)**	**T_{out} (°C)**	**Q_{ext} (MJ)**	**T_{LCZ} (°C)**	**ΔT**	**ε (%)**	**$\eta_{inst\ SP}$ (%)**
Independent heat extraction	BHE	0.014	10.9	22.8	12.40	28.4	11.9	68	16.6
	LHE	0.014	11.2	23.2	13.22	28.7	12.0	69	24.2
Simultaneous heat extraction	BHE	0.014	11.1	23.1	14.32	29.8	12.0	64	18.7
	LHE	0.014	11.4	23.7	14.64		12.3	67	

The temperature increases across the heat exchanger during the heat extraction process up to approximately 12°C in each test regardless of the heat exchange method used. This value is lower than that assumed in a theoretical study conducted by Date et al., 2013 who considered a minimum temperature difference of 20°C between inlet and outlet temperature in a heat extraction from the NCZ. This temperature difference would be required for heat transfer between the working fluid and the low temperature application. The difference between both values is due to the effectiveness of the heat exchangers. Date et al., 2013 assumed the inlet and outlet temperature of the working fluid as the temperature of the UCZ and the temperature of LCZ, respectively which means that the effectiveness of the heat exchanger is equal to 1. In this study, the effectiveness in winter conditions was an average of 65%, thus, the working fluid absorbed a significant amount of energy. This energy (12.4 and 13.2 MJ) corresponds to the heat extracted from the bottom and lateral heat exchangers, respectively. In the case of simultaneous heat extraction, the energy extracted was approximately 30 MJ. According to these values, the energy recovered in the simultaneous heat extraction was twice the value of independent heat extraction. Nevertheless, the LCZ temperature was kept constant during the simultaneous heat extraction because part of the energy was extracted from the NCZ. For this reason, the simultaneous extraction represents an increase in the energy extracted without causing a temperature decrease in the storage zone of the solar pond. The higher instantaneous efficiency was achieved when the heat extraction was performed with the LHE compared to the traditional method of heat extraction using the BHE (Table 1). Thus, the use of the LHE during cold months represents a substantial gain in instantaneous efficiency of approximately 50% compared with the BHE because part of the heat extracted comes from the NCZ instead of the LCZ. When the heat extraction was performed using both the lateral and bottom heat exchangers, the instantaneous efficiency achieved an intermediate value (19%).

The instantaneous efficiency of the solar pond during December 2013 is shown in Figure 5. As seen, the average instantaneous efficiency of the solar pond without heat extraction is approximately 16%. Indeed, the instantaneous efficiency increased when the heat extraction was performed using the LHE and both heat exchangers. Otherwise, heat extraction using the BHE did not improve the instantaneous efficiency of the solar pond.

Figure 5.

4.2 Heat extraction during a warm month (average daily maximum temperature in the range 20 to 28°C)

The heat extraction process during summer time was performed during July 2014. The LCZ temperature, the ambient temperature and the solar radiation during this month are plotted in Figure 6. The daily average solar radiation during this month was 25.7 MJ/m^2. The average maximum monthly ambient temperature was 28°C. The average daily LCZ temperature was practically constant (55°C). The maximum temperature achieved in the storage zone during this month was 58.5°C. The experimental conditions of heat extraction using both heat exchangers are collected in Table 2.

Figure 6.

Table 2. Working conditions, heat absorbed, effectiveness and instantaneous efficiency in heat extraction experiments during July 2014 (average daily maximum temperature in the range 20 to 28°C).

July 2014		**m (kg/s)**	**T_{in} (°C)**	**T_{out} (°C)**	**Q_{ext} (MJ)**	**T_{LCZ} (°C)**	**ΔT**	**ε (%**	**$\eta_{inst\ SP}$ (%)**
Independent heat extraction	BHE	0.014	29.5	51.7	24.2	56.4	22.2	82	8.8
	LHE	0.015	25.1	50.5	30.3	56.8	25.4	80	12.2
Simultaneous heat extraction	BHE	0.008	30.9	50.6	12.4	57.0	19.3	76	9.4
	LHE	0.0085	30.9	50.9	13.9		19.5	77	

Simultaneous heat extraction tests were performed with a total mass flow rate equivalent to that used for each heat exchanger separately. The inlet and outlet temperature were maintained constant during each heat extraction experiment. Moreover, the temperature of the LCZ was constant up to approximately 55°C. The LHE was able to extract heat at the same temperature than the BHE but with an instantaneous efficiency of approximately 12% representing a gain (relative percentage) of approximately 30% compared to the conventional method. The working fluid increased its temperature by 22.2°C (BHE) and 25.4°C (LHE) whereas this increase was approximately 20°C in the simultaneous heat extraction. The heat extracted ranged between 24 and 30 MJ for the three extraction methods, the LHE being the method that reported the higher amount of energy. The effectiveness was 82% and 80% when heat was extracted using BHE and

LHE, respectively. In simultaneous heat extraction, the effectiveness decreased to 76%. This behaviour is because the inlet temperature of the working fluid is increased during the experiment because of the higher ambient temperature during the summertime (average maximum monthly of 28°C), which leads to a lower capability to remove heat. This limitation was enhanced when both heat exchangers were used.

The instantaneous efficiency with and without heat extraction during the summer heat extraction experiments is shown in Figure 7. The average instantaneous efficiency of the solar pond without heat extraction is approximately 8%. The LHE reported a higher instantaneous efficiency (12.2%) than the BHE (8.8%). It should be noted that these values are lower compared to those reported during the winter tests. The instantaneous efficiency decreases in warmer months due to the temperature difference between the pond brine and the ambient temperature causing greater heat losses through the walls and bottom of the pond (Dehghan et al., 2013).

Figure 7.

4.3 Heat extraction during a moderately warm month (average daily maximum temperature in the range 10 to 20°C)

Two scenarios were considered during heat extraction experiments in autumn of 2014. First, the heat extraction was performed at a constant mass flow rate using both heat exchangers separately and near twice the mass flow rate in the simultaneously heat extraction during October 2014. Second, in November 2014, simultaneous heat extraction was performed at two different levels of mass flow rate, equivalent and double the value used by independent heat exchangers as is summarized in Table 3.

The daily average ambient and the LCZ temperatures during October and November 2014 are shown in Figure 8. The maximum daily solar radiation was 15.2 MJ/m^2 and 10.5 MJ/m^2 for October and November, respectively. The average monthly maximum ambient temperatures were 19.2°C and 13°C and the LCZ temperature decreased from 45°C to 37°C during October and to 29°C during November.

Figure 8.

Table 3. Working conditions, heat absorbed, effectiveness and instantaneous efficiency in heat extraction experiments during October and November 2014.

October 2014		**m(kg/s)**	**T_{in} (°C)**	**T_{out} (°C)**	**Q_{ext} (MJ)**	**T_{LCZ} (°C)**	**ΔT**	**ε (%)**	**$\eta_{inst\ SP}$ (%)**
Independent heat extraction	BHE	0.014	17.5	40.0	24.7	43.7	22.6	86	6.8
	LHE	0.014	17.3	38.1	23.8	42.9	20.8	81	10.8
Simultaneous heat extraction	BHE	0.011	20.6	40.4	18.0	44.5	20.1	84	8.7
	LHE	0.010	20.6	40.0	15.5		19.4	81	
November 2014		**m(kg/s)**	**T_{in} (°C)**	**T_{out} (°C)**	**Q_{ext} (MJ)**	**T_{LCZ} (°C)**	**ΔT**	**ε (%)**	**$\eta_{inst\ SP}$ (%)**
Independent heat extraction	BHE	0.017	15.5	31.3	20.4	35.5	15.8	79	5.3
	LHE	0.017	15.8	30.1	18.1	34.1	14.3	78	14.5
Simultaneous heat extraction (1)	BHE	0.009	16.8	30.6	10.5	36.4	13.8	71	6.9
	LHE	0.009	16.8	30.5	11.0		13.6	70	
Simultaneous heat extraction (2)	BHE	0.017	18.1	31.3	17.2	36.0	13.2	74	6.2
	LHE	0.018	18.1	29.9	16.7		11.9	66	

The working conditions of the heat extraction process during October and November 2014, the effectiveness of the heat extraction and the instantaneous efficiency of the solar pond are summarized in Table 3. The average temperature of the LCZ during this set of experiments was 43.7°C and 35.5°C for October and November, respectively.

The LHE reported the higher instantaneous efficiency (10.8%) during the test performed in October, representing a gain of approximately 58% compared to the BHE. Simultaneous heat extraction represented a total heat extracted of 33.5 MJ, which was higher than independent heat extraction using approximately the same mass flow rate in each heat exchanger as was observed during winter experiments (subsection 4.1). The heat extraction effectiveness (approximately 80%) was higher than that in winter and similar to the summer conditions.

The instantaneous efficiency of the solar pond with and without heat extraction during October and November are shown in Figure 9a. As seen, the average instantaneous efficiency of the solar pond without heat extraction was not constant due to the fluctuations in the solar radiation during this month with a maximum value of 7.7%. The instantaneous efficiency increased when the heat extraction was performed using the LHE (10.8%) followed by simultaneous extraction (8.7%). The extraction using the BHE reported the lower instantaneous efficiency (6.8%) during this month.

Figure 9.

The experiments performed during November followed the same trend observed during test performed in October. The average instantaneous efficiency of the solar pond without heat extraction was approximately 7% showing a decreasing trend at the end of the month due the cloud cover. The highest value of the instantaneous efficiency occurred when the heat was removed using the LHE (14.5%). The test using simultaneous heat extraction with a flow rate of 0.018 kg/s reported an instantaneous efficiency of 6.9% (heat extraction 1) and 6.2% when the flow rate was 0.035 kg/s (heat extraction 2) (Figure 9b). Increasing the mass flow rate did not represent a substantial increase in the instantaneous efficiency, as was observed during winter and summer conditions.

The instantaneous efficiency using LHE shows a value of 14.5%. This efficiency represents a gain of approximately 175% compared with the BHE. It can be related to a lower solar radiation during bottom extraction (223.4 MJ) instead of other heat extraction tests (the average of solar radiation was approximately 497.6 MJ). In winter, summer and early autumn conditions the solar radiation remained constant with average solar radiation values of approximately 228 MJ, 1456 MJ and 686 MJ, respectively.

The heat obtained when the heat extraction was performed using bottom and lateral heat exchangers separately was 20.4 MJ and 18.1 MJ, respectively. When the heat was removed using both heat exchangers the amount of energy extracted was dependent on the mass flow rate used. In the first case when the total mass flow rate was 0.018 kg/s, the heat obtained from the solar pond was 21.5 MJ. In the second case, when the mass flow rate was increased by a factor of about two (0.035 kg/s) the total heat obtained was 33.8 MJ. The performance of the system in this case was the same than in the other seasonal conditions and it confirms that using both heat exchangers can diminish the cooling effect in the storage zone compared to the independent heat extraction process.

The effectiveness of the heat exchangers in November was lower than in October or summer conditions and similar to winter conditions. The cooler months presented a lower efficiency than the warmer months. In this case, when the heat was removed using the bottom and the lateral heat exchanger independently, the effectiveness was 79% and 78%, respectively. The effectiveness of the simultaneous heat extraction was approximately 66% to 74%.

The temperature variations (ΔT) as a function of the solar pond depth from the beginning to the end of the heat extraction tests are shown in Figure 10. To compare the performance of the system without heat extraction, the day before the heat extraction test was included as a reference of the temperature variation. When heat extraction was performed using the BHE during winter, summer and autumn (Figures 10 a, d, g), the LCZ temperature decreased due to the heat removed in this zone, while the temperature the gradient zone was approximately constant near the temperature without heat extraction. It can also be observed that during winter conditions (Figure 10 g) the temperature difference is higher than during summer conditions (Figure 10 d). This is because the extracted energy is higher than the solar energy absorbed and stored by the pond.

Similar behaviour was reported for heat extraction by the LHE (Figures 10 b, e, h). For all of the experiments (winter, summer and autumn) a temperature variation was detected in the NCZ. The heat was removed from this zone and no significant temperature variation was observed in the LCZ. Finally, when heat extraction was performed by both heat exchangers, it was observed how the variation of temperature occurred both in the LCZ and in the NCZ. The difference in temperature was more pronounced in the cooler seasons (Figure 10 c, i, j) than in the warmer seasons (Figure 10 f) due to the high solar radiation and the greater amount of energy absorbed and stored, which compensated for the heat removed by both HE. The influence of flow rate on simultaneous heat extraction was evaluated during experiments in November. The temperature difference in NCZ is almost the same regardless of the mass flow rate used. In contrast, an increase of the mass flow rate in the LCZ represents an increase in the temperature difference, as seen in Figures 10 i and j.

The results reported in this study indicate that heat extraction from the NCZ has increased the efficiency of the energy extracted by a solar pond compared to the conventional method of heat extraction solely from the LCZ. However, it should be pointed out that heat extraction from the NCZ can affect the thermal gradient and in the end the stability of the solar pond. Leblanc et al., 2012 reported localised convective currents due to the cooling effect of the heat transfer fluid flowing in the heat exchanger tubes when heat extraction were performed from the NCZ even that no effect on the density profile was observed, similar behaviour was reported in this work (Figure 1). Moreover, Date et al., 2011 indicated that this heat extraction method can also result in a smaller temperature gradient in the upper region of the gradient layer, which can lead to a combined effect of instabilities due to local temperature gradients as well as mixing due to wind action on the surface. Then, it is suggested that the stability of the salinity gradient must be evaluated and monitored in a long-term heat extraction from the NCZ in order to avoid a degradation of the thermal gradient.

Figure 10.

5. Conclusions

The performance of heat extraction from a salinity-gradient solar pond by two different methods in three weather scenarios with different daily ambient temperature conditions was evaluated. Two in-pond heat exchangers located at the bottom and at the lateral area of the pond were used independently and simultaneously. The results indicated that the instantaneous efficiency of the solar pond increases when the heat extraction was performed by the LHE regardless the weather conditions and compared with the traditional method of heat extraction from the LCZ. It was clearly seen how the instantaneous efficiency shows higher values during the cooler seasons compared with the warmer seasons. This behaviour during cold temperature conditions represents a substantial gain in instantaneous efficiency above 50% compared with the traditional method of heat extraction. In warm conditions, the LHE reported a gain of approximately 30%. The use of both heat exchangers supposes a slight gain in the instantaneous efficiency of the solar pond compared with the efficiency obtained in the BHE. The main advantage in the use of both heat exchangers in the heat extraction process is that the pond can deliver the same quantity of energy working at a lower flow rate. It means that the LCZ is capable of preserving more stored thermal energy using both heat exchangers than in the case of independent heat extraction. Therefore, this new heat-extraction method may represent an advantage in preserving the thermal gradient of the solar pond and consequently the stability of the salinity gradient.

However in long term heat extraction, local temperature gradients can represent a source of instabilities and the gradient degradation making necessary a continuous analysis of the solar pond stability.

Finally, lower values of effectiveness were reported for heat extraction during cooler seasons compared with warmer seasons. During the heat extraction test conducted in December 2013, the effectiveness reached values above 60%, whereas the effectiveness of the heat exchanger in July, October and November showed values of approximately 80%.

Nomenclature

$j_{m\,f}$ is the mass flux of the heat transfer fluid (kg/(m^2·s)),

$C_{p\,f}$ is the specific heat capacity of the heat transfer fluid (J/kg·°C),

T_{of}^{τ} is the outlet temperature of the heat transfer fluid (°C)

$T_{i\,f}^{\tau}$ is the inlet temperature of the heat transfer fluid (°C)

$\Delta\tau$ is the time increment of the heat extraction process (s)

X_{lcz} is the path length of light in the solar pond to the end of the LCZ (m)

A_{sp} is the surface area of solar pond (m^2)

ρ_{lcz} is the density of the brine in the LCZ (kg/m^3)

$C_{p\,lcz}$ is the specific heat capacity of the brine solution in the LCZ (J/kg·°C)

$T_{lcz}^{\tau-1}$ is the LCZ temperature at the beginning of the heat extraction process (°C)

T_{lcz}^{τ} is the LCZ temperature at the end of the heat extraction process (°C)

$\eta_{inst\,SP}$ is the instantaneous efficiency of the solar pond

$\overline{H}$ is the total energy of the solar radiation incident on the horizontal surface of the pond (MJ/m^2)

S is the salt concentration (kg/m^3)

ε is the effectiveness of the heat exchanger

ΔE_{lcz}^{τ} is the instantaneous energy change in the energy content

Abbreviations

SGSP: salinity-gradient solar pond

UCZ: upper convective zone

LCZ: low convective zone

NCZ: non-convective zone

LHE: lateral heat exchanger

BHE: bottom heat exchanger

Acknowledgments

The authors gratefully acknowledge personnel from Solvay Martorell facilities for practical assistance, especially to M. Giménez and C. Aladjem for their valuable cooperation. This study has been supported by the Zero discharge project (CTQ2011-26799) and the Waste2Product project (CTM2014-57302-R) financed by Ministry of Science and Innovation (MINECO, Spain) and the Catalan government (project ref.2014SGR050).

6. References

Akbarzadeh, A., Andrews, J., Golding, P., 2005. Solar Pond Technologies: A review and Future Directions. Adv. Sol. Energy 233–294.

Andrews, J., Akbarzadeh, a., 2005. Enhancing the thermal efficiency of solar ponds by extracting heat from the gradient layer. Sol. Energy 78, 704–716. doi:10.1016/j.solener.2004.09.012

Bansal, P.K., Kaushik, N.D., 1981. Salt gradient stabilized solar pond collector. Energy Convers. Manag. 21, 81–95.

Bozkurt, I., Karakilcik, M., 2015. The effect of sunny area ratios on the thermal performance of solar ponds. Energy Convers. Manag. 91, 323–332. doi:10.1016/j.enconman.2014.12.023

Date, A., Yaakob, Y., Date, A., Krishnapillai, S., Akbarzadeh, A., 2013. Heat extraction from Non-Convective and Lower Convective Zones of the solar pond: A transient study. Sol. Energy 97, 517–528. doi:10.1016/j.solener.2013.09.013

Dehghan, A. a., Movahedi, A., Mazidi, M., 2013. Experimental investigation of energy and exergy performance of square and circular solar ponds. Sol. Energy 97, 273–284. doi:10.1016/j.solener.2013.08.013

El-Sebaii, a. a., Ramadan, M.R.I., Aboul-Enein, S., Khallaf, a. M., 2011. History of the solar ponds: A review study. Renew. Sustain. Energy Rev. 15, 3319–3325. doi:10.1016/j.rser.2011.04.008

Hull, J.R., Nielson, C.E., Golding, R., 1989. Salinity Gradient Solar Ponds.

Jaefarzadeh, M.R., 2006. Heat extraction from a salinity-gradient solar pond using in pond heat exchanger. Appl. Therm. Eng. 26, 1858–1865. doi:10.1016/j.applthermaleng.2006.01.022

Karakilcik, M., Dincer, I., Rosen, M. a., 2006. Performance investigation of a solar pond. Appl. Therm. Eng. 26, 727–735. doi:10.1016/j.applthermaleng.2005.09.003

Kho, T.H., Hawlader, M.N.A., Ho, J.C., Wijeysundera, N.E., 1991. Design and performance evaluation of a solar pond for industrial process heating. Int. J. Sol. Energy 10, 83–101.

Kumar, A., Kishore, V.V.N., 1999. Construction and operational experience of a 6000 M2 solar pond at kutch, India. Sol. Energy 65, 237–249.

Leblanc, J., Akbarzadeh, A., Andrews, J., Lu, H., Golding, P., 2011. Heat extraction methods from salinity-gradient solar ponds and introduction of a novel system of heat extraction for improved efficiency. Sol. Energy 85, 3103–3142. doi:10.1016/j.solener.2010.06.005

Leblanc, J., Andrews, J., Akbarzadeh, A., 2010. Low-temperature solar-thermal multi-effect evaporation desalination systems. Int. J. Energy Res. 34, 393–403.

Nielsen, C.E., 1980. No Title. Sol. Energy Technol. Handb.

Ranjan, K.R., Kaushik, S.C., 2014. Thermodynamic and economic feasibility of solar ponds for various thermal applications: A comprehensive review. Renew. Sustain. Energy Rev. 32, 123–139. doi:10.1016/j.rser.2014.01.020

Tabor, H., Weinberger, Z., 1981. Non-Convecting Solar Ponds.

Tabor, H.Z.., Doron, B.., 1990. The Beith Ha'Arava 5 MW(e) Solar Pond Power Plant (SPPP)-Progress report. Sol. Energy 45, 247–253.

Tundee, S., Terdtoon, P., Sakulchangsatjatai, P., Singh, R., Akbarzadeh, A., 2010. Heat extraction from salinity-gradient solar ponds using heat pipe heat exchangers. Sol. Energy 84, 1706–1716. doi:10.1016/j.solener.2010.04.010

Valderrama, C., Gibert, O., Arcal, J., Solano, P., Akbarzadeh, A., Larrotcha, E., Cortina, J.L., 2011. Solar energy storage by salinity gradient solar pond: Pilot plant construction and gradient control. Desalination 279, 445–450. doi:10.1016/j.desal.2011.06.035

Wang, Y.F., Akbarzadeh, A., 1982. A study on the transient behaviour of solar ponds. Energy 7, 1005–1017.

Weinberger, H., 1964. The physics of the solar pond. Sol. Energy 8, 45–56.

Xu, H., Sandoval, J.S., Lu, H., Ybarra, A., Golding, P., Swift, A., 1993. Operating experience with the El Paso solar pond. Proc., 3rd Int. Conf. Prog. Sol. Ponds 69–84.

Yaakob, Y., Date, A., Akbarzadeh, A., (2011). Heat extraction from gradient layer using external heat exchangers to enhance the overall efficiency of solar ponds. IEEE First Conference on Clean Energy and Technology (CET).

Zangrando, F., 1980. A simple method to establish salt gradient solar ponds. Sol. Energy 25, 467–470.

Figure

Figure captions

Figure 1. Season density profile as a function of the Solar Pond height (m) between winter 2013 and autumn 2014.

Figure 2. a) Martorell solar pond pilot plant image including photovoltaic cells and b) the cooler system (HRS024-AF-20 2.1kW SMC) used on the heat extraction experiments.

Figure 3. a) Overview of the lateral (730 m) and bottom (250 m) heat exchangers in the pilot plant and scheme of the heat extraction by b) lateral heat exchanger and c) the bottom heat exchanger.

Figure 4. Average daily ambient temperature, LCZ temperature, and solar radiation during December 2013 a cold month (maximum daily average temperature in the range 5 to 10 °C).

Figure 5. Instantaneous efficiency of solar pond during December 2013 (average daily maximum temperature in the range 5 to 10 °C).

Figure 6. Average daily ambient temperature, LCZ temperature and average daily solar radiation during July 2014 (average daily maximum temperature in the range 20 to 28 °C).

Figure 7. Instantaneous efficiency of solar pond during July 2014 (average daily maximum temperature in the range 20 to 28 °C).

Figure 8. Average daily ambient temperature, LCZ temperature and average daily solar radiation during a) October and b) November 2014.

Figure 9. Instantaneous efficiency of solar pond during a) October and b) November 2014.

Figure 10. Temperature differences as function of the solar pond depth during the heat extraction test using a) BHE December 2013, b) LHE December 2013, c) BHE + LHE December 2013, d) BHE July 2014, e) LHE July 2014, f) BHE + LHE July 2014, g) BHE November 2014, h) LHE November 2014, i) BHE + LHE (0.018 kg/s = 0.5 L/min) November 2014 and j) BHE + LHE (0.035 kg/s = 1.0 L/min) November 2014.

Figure

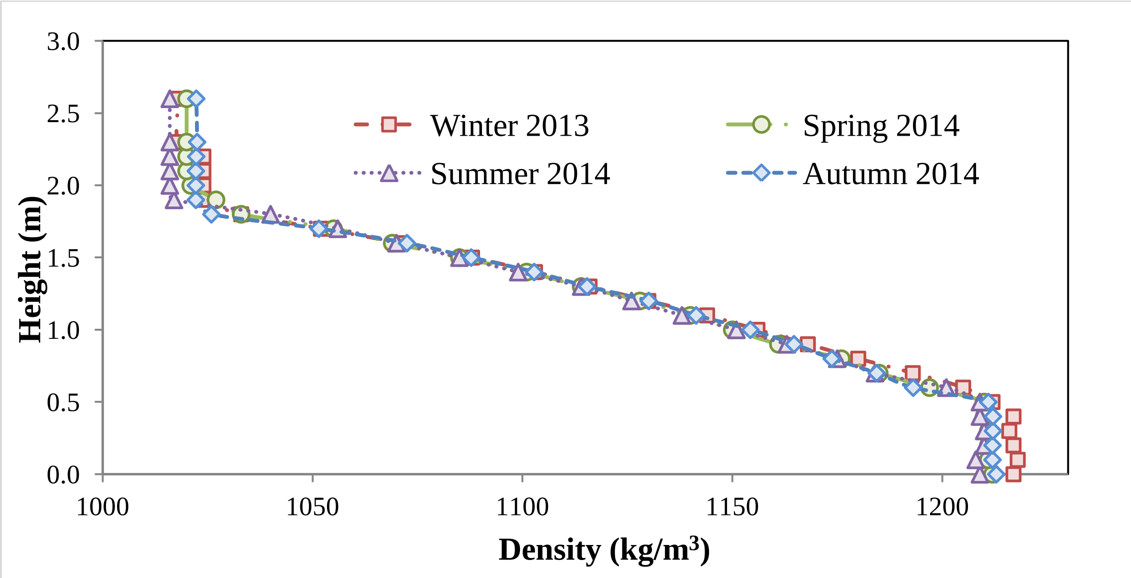

Figure 1.

Figure 2.

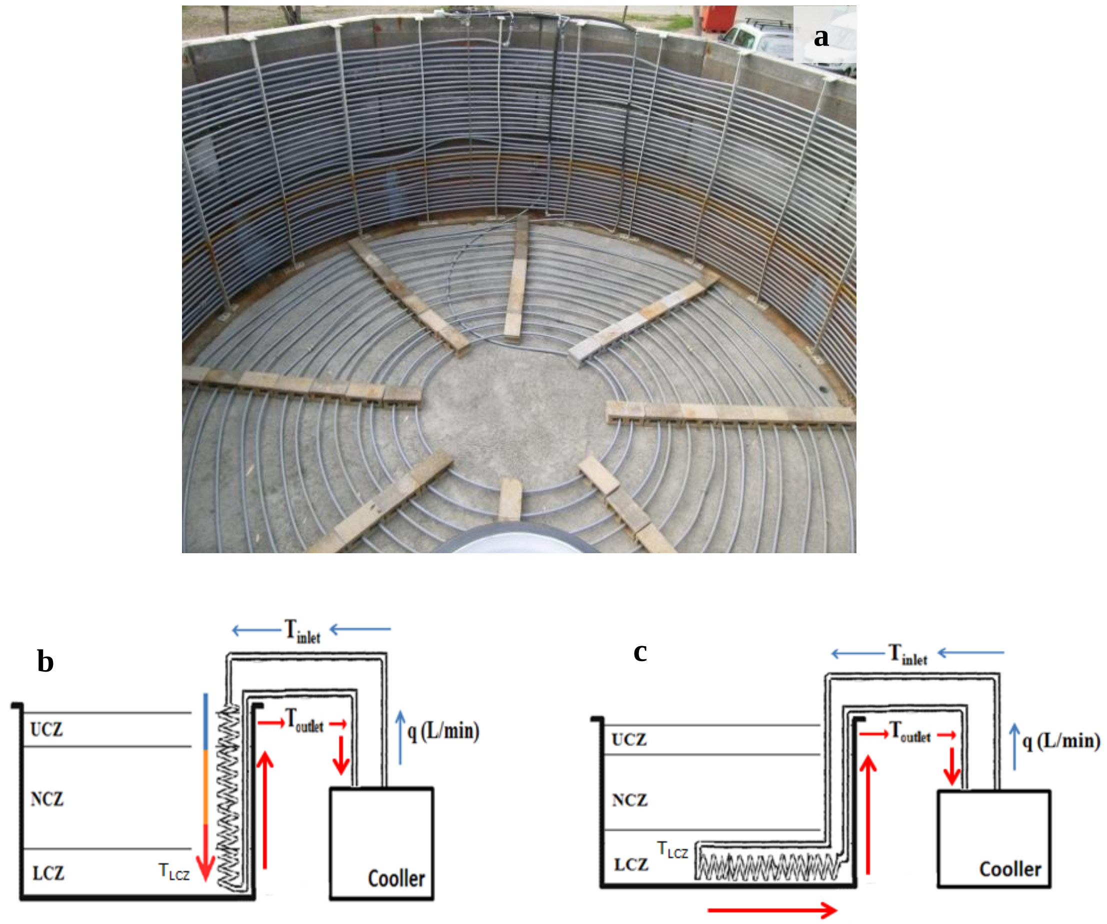
a
b
T_inlet
UCZ
NCZ
LCZ
T_LCZ
T_outlet
q (L/min)
Cooller
c
T_inlet
UCZ
NCZ
LCZ
T_LCZ
T_outlet
q (L/min)
Cooller

Figure 3.

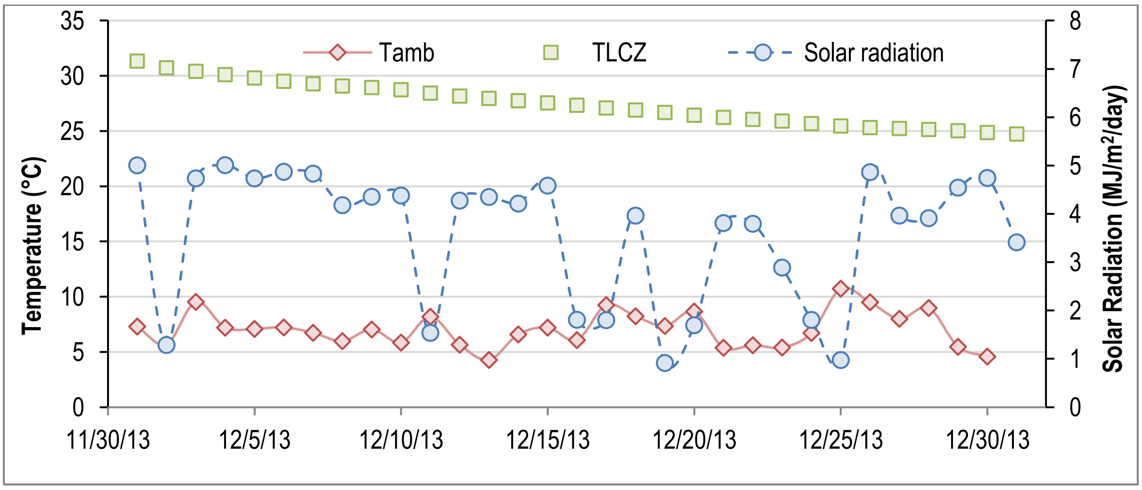
Tamb
TLCZ
Solar radiation
Temperature (°C)
Solar Radiation (MJ/m2/day)
35
30
25
20
15
10
5
0
8
7
6
5
4
3
2
1
0
11/30/13
12/5/13
12/10/13
12/15/13
12/20/13
12/25/13
12/30/13

Figure 4.

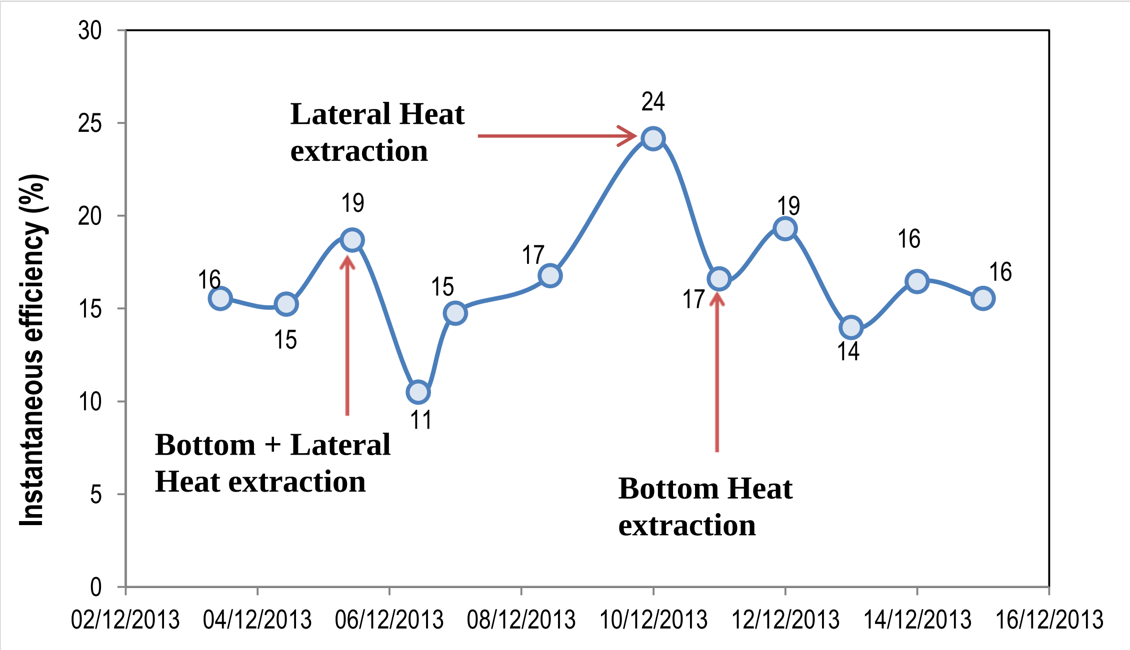

Instantaneous efficiency (%)
30
25
20
15
10
5
0
02/12/2013
04/12/2013
06/12/2013
08/12/2013
10/12/2013
12/12/2013
14/12/2013
16/12/2013
16
15
19
11
15
17
24
17
19
14
16
16
Lateral Heat extraction
Bottom + Lateral Heat extraction
Bottom Heat extraction

Figure 5.

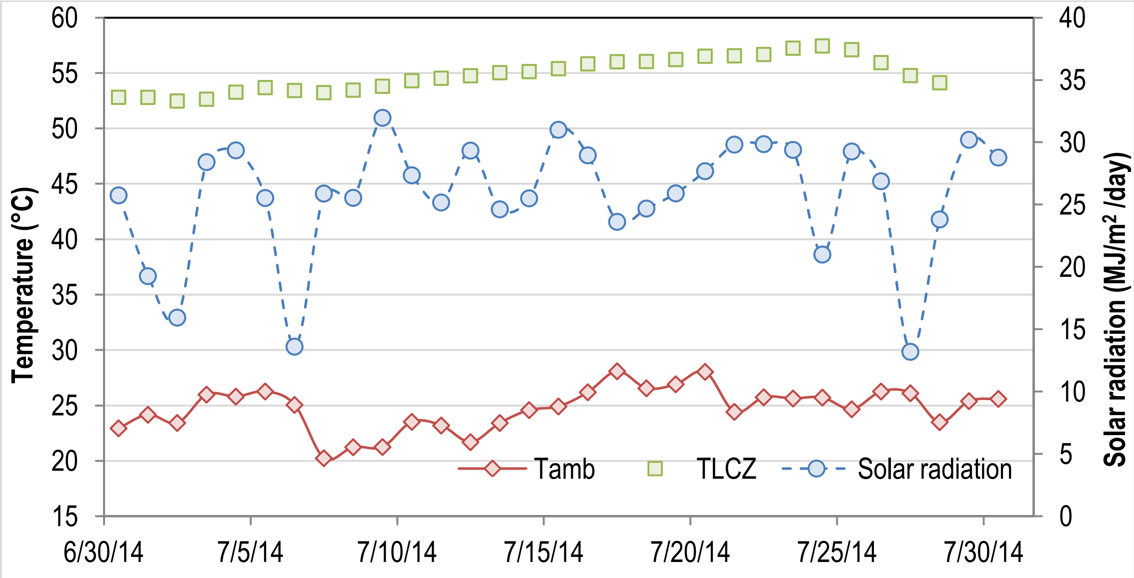

60
55
50
45
40
35
30
25
20
15
Temperature (°C)
40
35
30
25
20
15
10
5
0
Solar radiation (MJ/m² /day)
6/30/14
7/5/14
7/10/14
7/15/14
7/20/14
7/25/14
7/30/14
Tamb
TLCZ
Solar radiation

Figure 6.

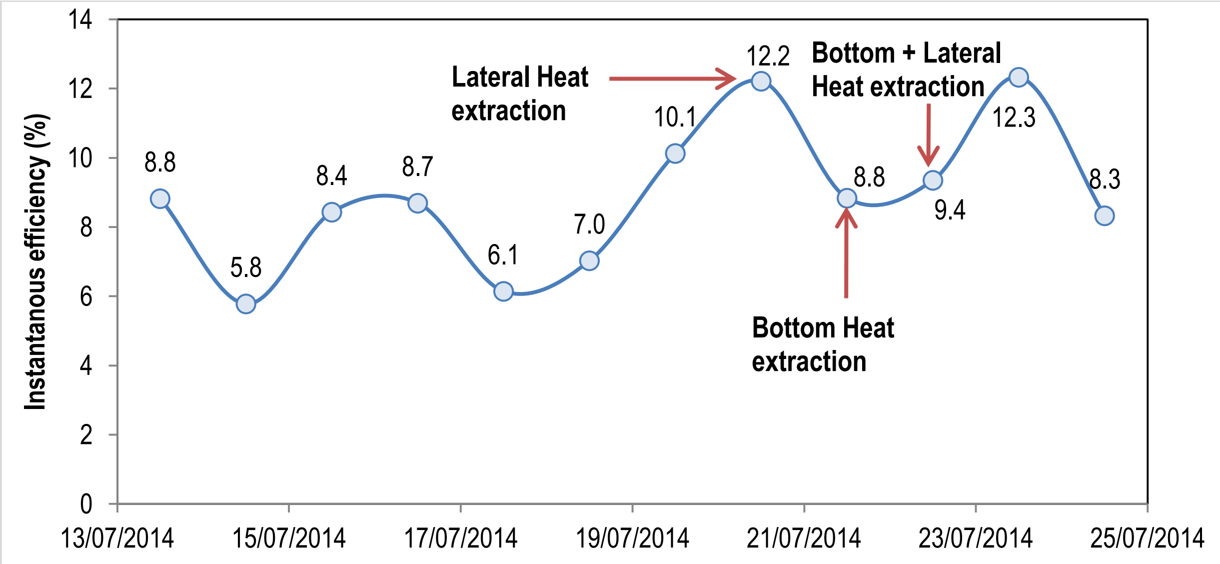
Instantanous efficiency (%)
0
2
4
6
8
10
12
14
13/07/2014
15/07/2014
17/07/2014
19/07/2014
21/07/2014
23/07/2014
25/07/2014
8.8
5.8
8.4
8.7
6.1
7.0
10.1
12.2
8.8
9.4
12.3
8.3
Lateral Heat extraction
Bottom + Lateral Heat extraction
Bottom Heat extraction

Figure 7.

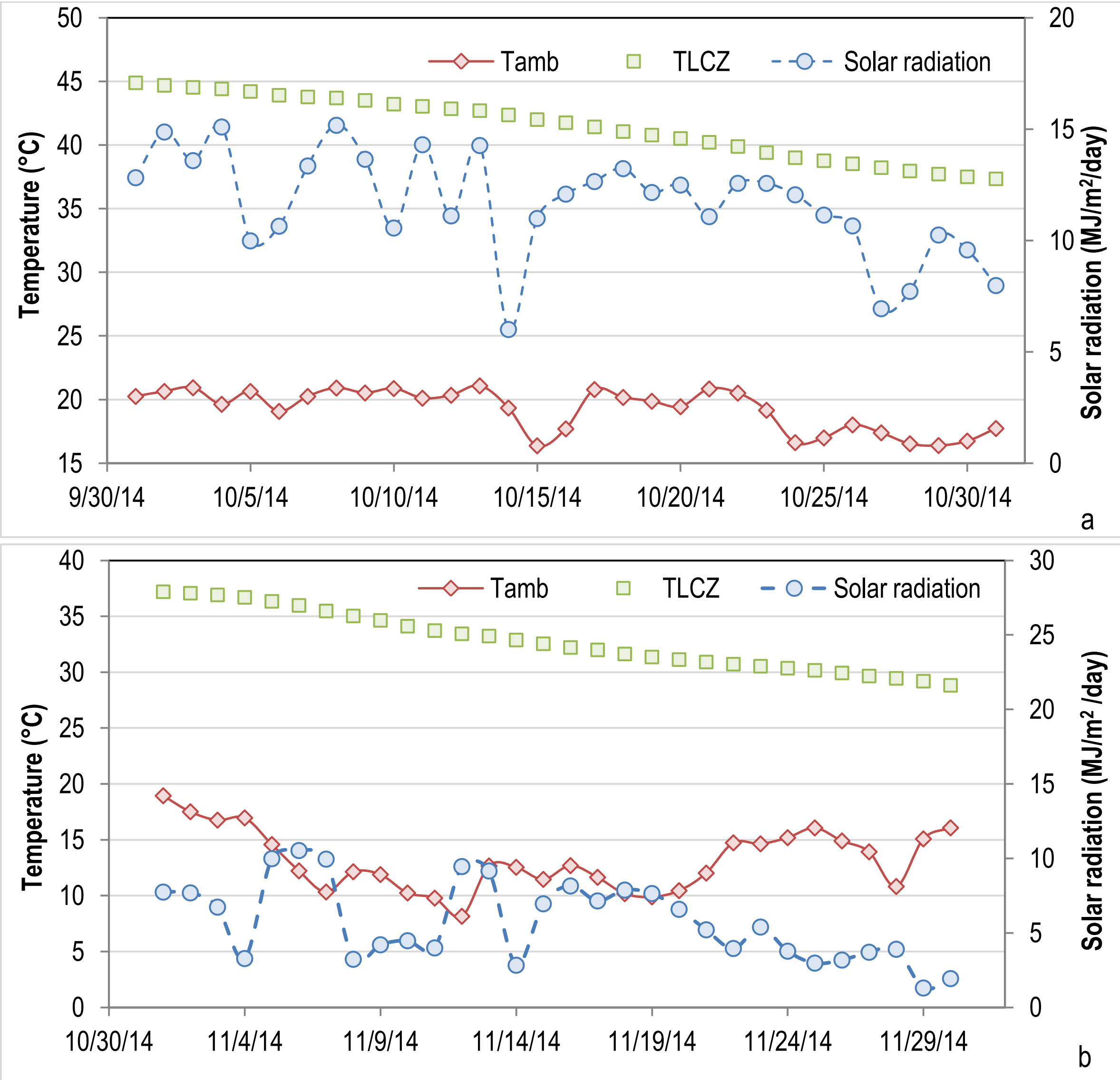

Tamb
TLCZ
Solar radiation
Temperature (°C)
Solar radiation (MJ/m2/day)
9/30/14
10/5/14
10/10/14
10/15/14
10/20/14
10/25/14
10/30/14
a
11/4/14
11/9/14
11/14/14
11/19/14
11/24/14
11/29/14
b

Figure 8.

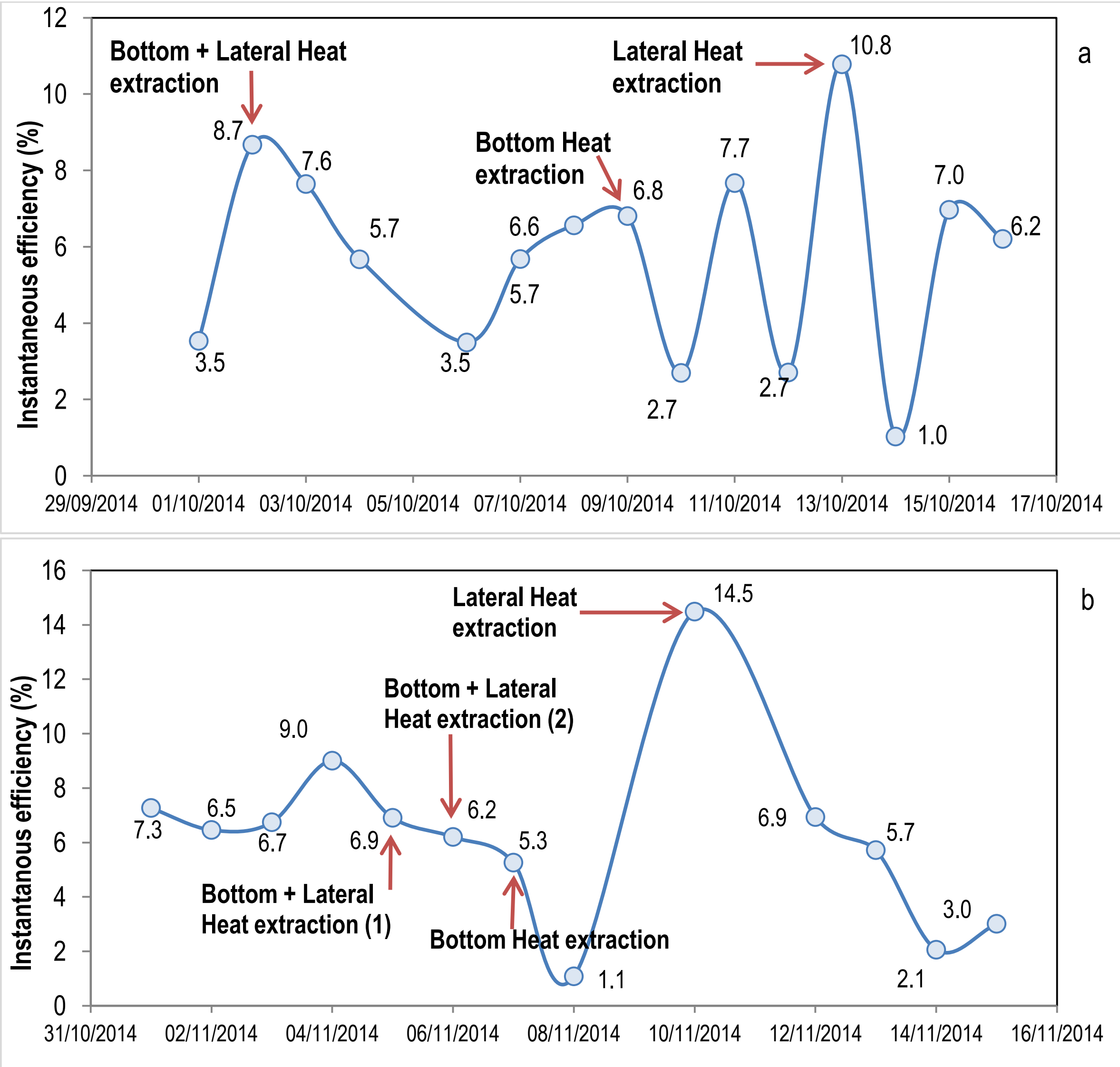
a
Instantaneous efficiency (%)
Bottom + Lateral Heat extraction
Lateral Heat extraction
Bottom Heat extraction
3.5
8.7
7.6
5.7
3.5
5.7
6.6
6.8
2.7
7.7
2.7
10.8
1.0
7.0
6.2
29/09/2014
01/10/2014
03/10/2014
05/10/2014
07/10/2014
09/10/2014
11/10/2014
13/10/2014
15/10/2014
17/10/2014
b
Instantanous efficiency (%)
Lateral Heat extraction
Bottom + Lateral Heat extraction (2)
Bottom + Lateral Heat extraction (1)
Bottom Heat extraction
7.3
6.5
6.7
9.0
6.9
6.2
5.3
1.1
14.5
6.9
5.7
2.1
3.0
31/10/2014
02/11/2014
04/11/2014
06/11/2014
08/11/2014
10/11/2014
12/11/2014
14/11/2014
16/11/2014

Figure 9.

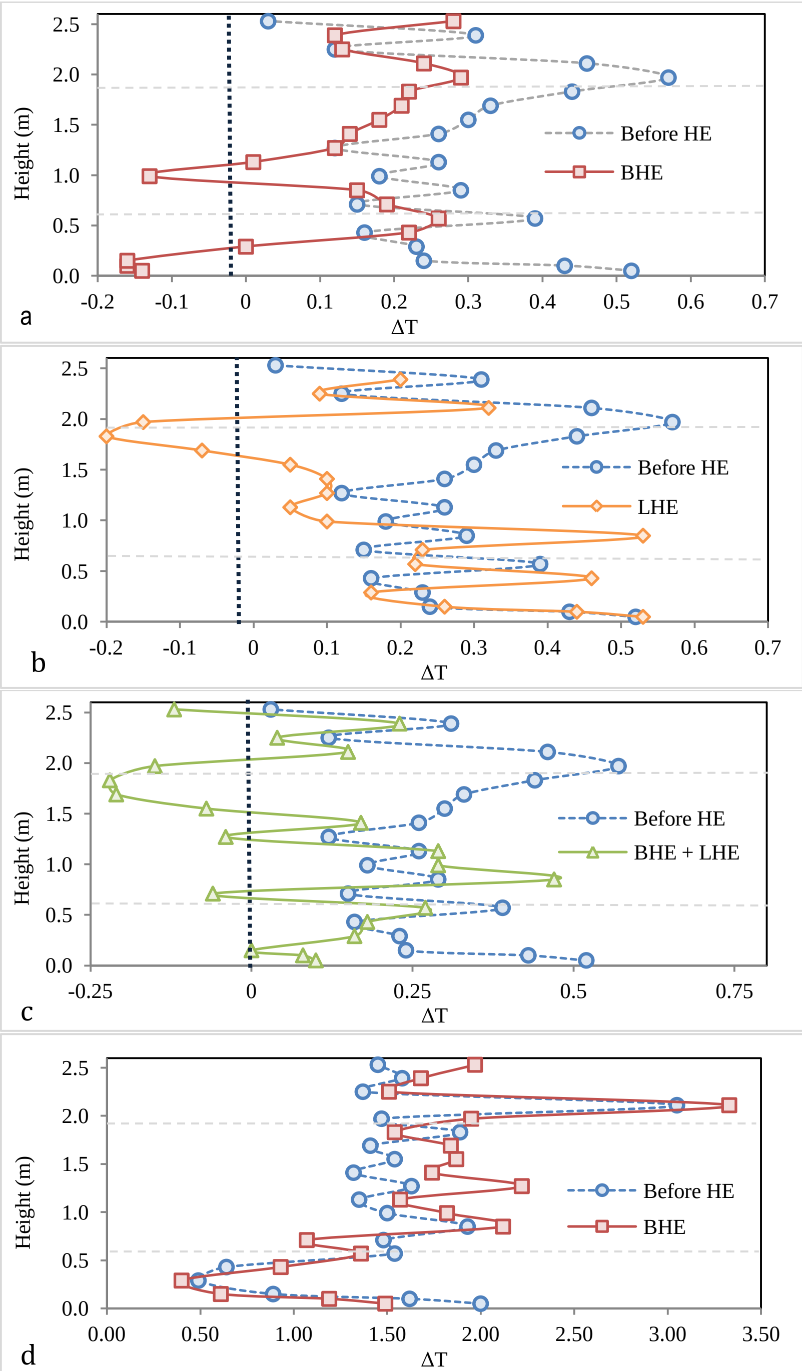
a
b
c
d
Height (m)
ΔT
Before HE
BHE
LHE
BHE + LHE

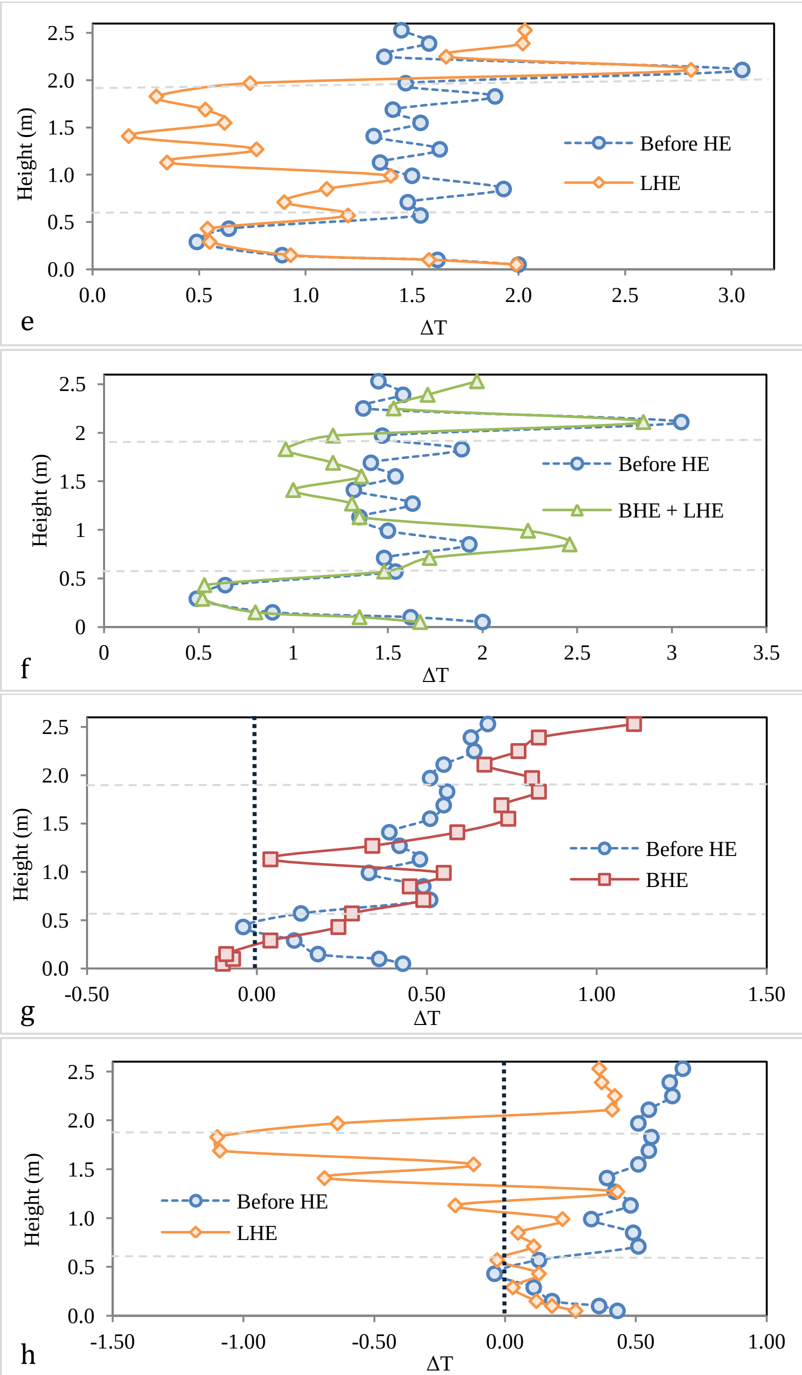

e
Height (m)
ΔT
Before HE
LHE
f
Height (m)
ΔT
Before HE
BHE + LHE
g
Height (m)
ΔT
Before HE
BHE
h
Height (m)
ΔT
Before HE
LHE

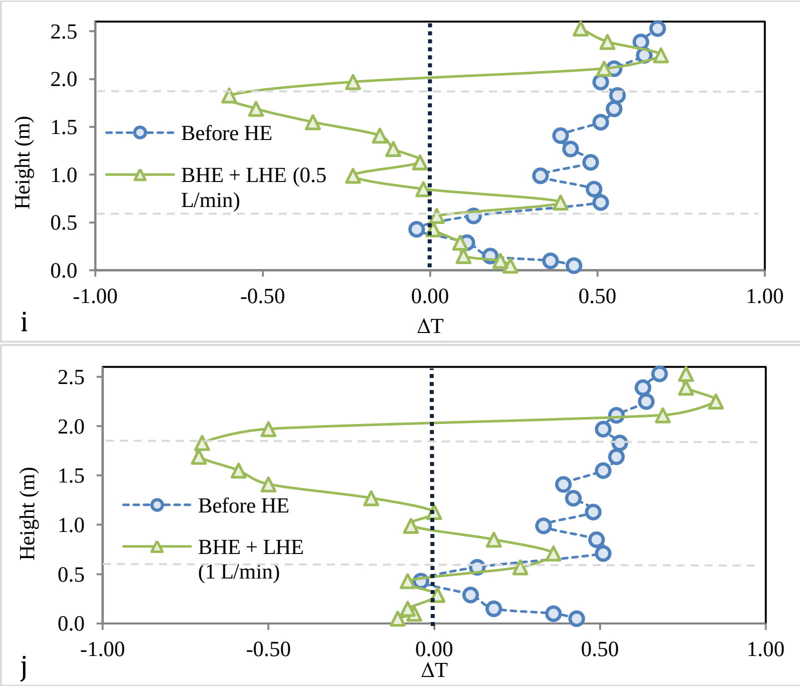
2.5
2.0
1.5
1.0
0.5
0.0
Height (m)
Before HE
BHE + LHE (0.5 L/min)
-1.00
-0.50
0.00
0.50
1.00
ΔT
i
2.5
2.0
1.5
1.0
0.5
0.0
Height (m)
Before HE
BHE + LHE (1 L/min)
-1.00
-0.50
0.00
0.50
1.00
ΔT
j

Figure 10.